Meshfree First-order System Least Squares

Hugh R. MacMillan[1,*], Max D. Gunzburger[2] and John V. Burkardt[3]

[1] *Department of Mathematical Sciences, Clemson University, Clemson,*
SC 29634-0975, USA.
[2] *School of Computational Science, Florida State University, Tallahassee,*
FL 32306-4120, USA.
[3] *Advanced Research Computing, Virginia Tech University, Blacksburg,*
VA 24061-0123, USA.

Abstract. We prove convergence for a meshfree first-order system least squares (FOSLS) partition of unity finite element method (PUFEM). Essentially, by virtue of the partition of unity, local approximation gives rise to global approximation in $H(div) \cap H(curl)$. The FOSLS formulation yields local *a posteriori* error estimates to guide the judicious allotment of new degrees of freedom to enrich the initial point set in a meshfree discretization. Preliminary numerical results are provided and remaining challenges are discussed.

AMS subject classifications: 65N30, 65N50
Key words: Meshfree methods, first-order system least squares, adaptive finite elements.

1. Introduction

1.1. Summary

Interest remains in avoiding the proper tessellation of a computational domain used to solve partial differential equations, especially in the context of moving meshfree, or meshless, particle methods. However, as will be made clear, the flexibility inherent to using merely the cover of a domain does not come without cost. A number of mostly-related meshfree approaches have been proposed, yielding a variety of approximation spaces from which to choose. For example, consider the diffuse element method (DEM), element free Galerkin (EFG), finite point method (FPM), HP clouds, meshfree local Petrov Galerkin (MLPG), smooth particle hydrodynamics (SPH), moving least squares SPH (ML-SPH), material-point method (MPM), partition of unity finite element method (PUFEM), reproducing kernel particle method (RKPM); see [1, 2] for a classification and review. Below, we employ the partition unity (PU) approach, given its flexibility and local nature, to discretize the prototypical first-order system least-squares (FOSLS) formulation for Poisson's equation. This synthesis can be generalized to existing FOSLS formulations of more

---

*Corresponding author. *Email address:* `hmacmil@clemson.edu` (H. R. MacMillan)

complicated PDE systems. Since the FOSLS formulation presents local a posteriori error estimates to guide adaptive enrichment of an initially-sparse point set, the synthesis may enhance the utility of meshfree methods.

Below, after a brief discussion about meshfree methods, we introduce FOSLS and a vector PUFEM discretization. Then, convergence is proved from assumptions about the local approximation spaces defined on each patch used to cover the domain. Finally, several numerical examples are provided.

1.2. Meshfreedom

The notion of altogether avoiding a mesh requires some clarification. First, a set of points in a domain, along with an associated covering of the domain, must be chosen. Given generic specifications for this covering, such as the density used in point set selection and the degree of overlap, a provision of points and their associated patches can be supplied probabilistically, without use of a background mesh [3]. However, enrichment of an initially sparse (or coarse) point set nevertheless entails relaxation of the new point set, in concert with updating the associated cover. While explicit retriangulation is thus avoided, significant refinement costs persist to ensure that both point placement and patch size are suitable.

Integration during assembly of the discrete problem leads to a second unavoidable computational cost. In lieu of a tessellation, integration over each intersecting pair of patches entails defining quadrature points either locally, in a consistent and efficient manner, or globally, appealing to some background mesh. Below we simply use circular patches Ω_i to cover a domain $\Omega \subset \mathbb{R}^2$. Rather than perform quadrature on each individual lens, $\Omega_i \cap \Omega_j$, which would yield a symmetric linear system, it is more efficient to simply set a quadrature rule on each Ω_i. Of course, this leads to an asymmetric system due to inexact integration, i.e., A_{ij} is computed using quadrature on Ω_i while A_{ji} is computed using quadrature on Ω_j.

Our approach is truly meshfree in the sense that integration is performed according to neighbor connectivity, point locations, and neighboring support radii, not according to the elements of a tessellation. No background mesh is utilized. As a result, adding and/or moving individual points is unencumbered by the need to re-tessellate the domain. This flexibility comes with less-efficient assembly of the discrete problem, primarily because there are many more regions of overlap, $\Omega_i \cap \Omega_j$, than there are elements of a comparable tessellation. This cost is compounded by the partition of unity construction, which yields conforming discretizations at the expense of pointwise conditions on the degree of overlap; e.g., requiring that each point be covered by at least three elements of the cover, $\#\{j | \Omega_i \cap \Omega_j \neq \emptyset\}$ approaches 30 in Fig. 1.

2. A FOSLS partition of unity method

FOSLS has been applied to far more difficult PDE systems than the simplistic elliptic problem considered below [4]. As a methodology, it is only distinct from least-squares (LS) in that a residual on vorticity, or the curl of velocity, is introduced in lieu of solving for

pressure; the latter is the common velocity-pressure formulation, while the former leads to approximation of velocity with respect to $H(div) \cap H(curl)$.

2.1. Flux-vorticity formulation

Consider the prototypical first-order system,

$$-\nabla \cdot \mathbf{u} = f \qquad \text{in } \Omega, \tag{2.1}$$

$$\nabla \times \mathbf{u} = \mathbf{0} \qquad \text{in } \Omega, \tag{2.2}$$

$$\mathbf{n} \cdot \mathbf{u} = 0 \qquad \text{on } \Gamma_N, \tag{2.3}$$

$$\boldsymbol{\tau} \cdot \mathbf{u} = \mathbf{0} \qquad \text{on } \Gamma_D, \tag{2.4}$$

where $\mathbf{u} \in H(div; \Omega) \cap H(\mathbf{curl}; \Omega)$ and $f \in L^2(\Omega)$. The simplest FOSLS (L^2) approach is to formulate the solution of system (2.1-2.4) as the minimizer of the interior functional

$$\mathscr{J}(\mathbf{u}; f) := \left(\|\nabla \cdot \mathbf{u} + f\|_{0,\Omega}^2 + \|\nabla \times \mathbf{u}\|_{0,\Omega}^2 \right)^{1/2}. \tag{2.5}$$

By design [4], this functional provides a norm on the space

$$\mathbf{W} = \left\{ \mathbf{v} \in H(div; \Omega) \cap H(curl; \Omega) \mid \mathbf{n} \cdot \mathbf{v} = 0 \text{ on } \Gamma_N, \ \boldsymbol{\tau} \cdot \mathbf{v} = \mathbf{0} \text{ on } \Gamma_D, \ \text{and} \int_{\Gamma_D} \boldsymbol{\tau} \cdot \mathbf{v} = \mathbf{0} \right\}.$$

That is,

$$\|\mathbf{v}\|_{\mathbf{W}} := \mathscr{J}(\mathbf{v}; 0, 0) = \sqrt{\langle \mathscr{L}\mathbf{v}, \ \mathscr{L}\mathbf{v} \rangle_{0,\Omega}}, \tag{2.6}$$

where

$$\mathscr{L} = \begin{pmatrix} -\nabla \cdot & 0 \\ 0 & \nabla \times \end{pmatrix}.$$

Note that the $(L^2(\Omega))^2$-innerproduct is conducted componentwise. Hence, solving for

$$\mathbf{u} = \arg\min_{\mathbf{v} \in \mathbf{W}} \mathscr{J}(\mathbf{v}; f) \tag{2.7}$$

is equivalent to minimizing error in the $\mathbf{W}$-norm. As is standard, defining functionals

$$\mathscr{F}(\mathbf{u}, \mathbf{v}) = \langle \mathscr{L}\mathbf{u}, \mathscr{L}\mathbf{v} \rangle_{0,\Omega}, \tag{2.8}$$

$$\ell(\mathbf{v}) = \langle (f \quad \mathbf{0})^t, \mathscr{L}\mathbf{v} \rangle_{0,\Omega}. \tag{2.9}$$

leads to a variational form of minimization problem (2.7):

Find $\mathbf{u} \in \mathbf{W}$ such that $\quad \mathscr{F}(\mathbf{u}, \mathbf{v}) = \ell(\mathbf{v}) \quad$ for all $\mathbf{v} \in \mathbf{W}$. $\tag{2.10}$

Motivation for this approach is two-fold. First, functional equivalence to an H^1-like norm implies optimal performance of multigrid methods in solving the resulting discrete problem. Furthermore, *a posteriori* $\mathbf{W}$-norm error estimates follow simply from evaluating the FOSLS functional given a computed solution. In [5], a meshfree LS formulation of

steady incompressible viscous flow is presented that uses a background mesh for integration and employs RKPM to achieve exact approximation of quadratic functions defined on the entire domain. We have chosen to avoid any background mesh and focus on retaining the capacity to enhance a given mesh locally through direct appeal to FOSLS a posteriori error estimates.

We now establish convergence for problem (2.10) when using a vector partition of unity to define a discrete subspace of $\mathbf{W}$. We only consider $\Omega \subset \mathbb{R}^2$ and use the notation $\nabla^{\perp} \cdot \mathbf{u} = \mathbf{k} \cdot (\nabla \times \mathbf{u})$, but extension to 3-D is straightforward. Non-homogeneous boundary conditions can be handled through standard lifting techniques or by adding appropriate boundary terms to (2.5). As will be illustrated, the latter gives rise questions as to the implementation of Sobolev norms on boundary spaces.

2.2. Vector PU Discretization

Briefly, a scalar partition of unity discretization involves first choosing a set of points in the domain, $\{\mathbf{z}_i\}_{i=1}^N$, and then determining corresponding supports, Ω_i, to constitute a cover, $\mathscr{C} = \{ \{\Omega_i\}_{i=1}^N \mid \cup_{i=1}^N \Omega_i \supset \Omega \}$. Next, a smooth compactly supported "window function" is chosen from which a Shephard partition of unity, subordinate to $\mathscr{C}$, is constructed. Analogous to standard p-refinement, local approximation spaces on each support can then be formed to improve approximation accuracy.

As discussed in [3], we determine a point set $\{\mathbf{z}_i\}_{i=1}^N = \{(x_i, y_i)\}_{i=1}^N$ along with associated radii $\{r_i\}_{i=1}^N$ to determine $\mathscr{C} = \{\Omega_i\}_{i=1}^N$ according to

$$\Omega_i = \{\mathbf{z} \in \mathbb{R}^2 \mid |\mathbf{z} - \mathbf{z}_i| \le r_i\} .$$

Fig. 1 illustrates the connectivity of neighboring patches for such a cover, given a point set with uniform density.
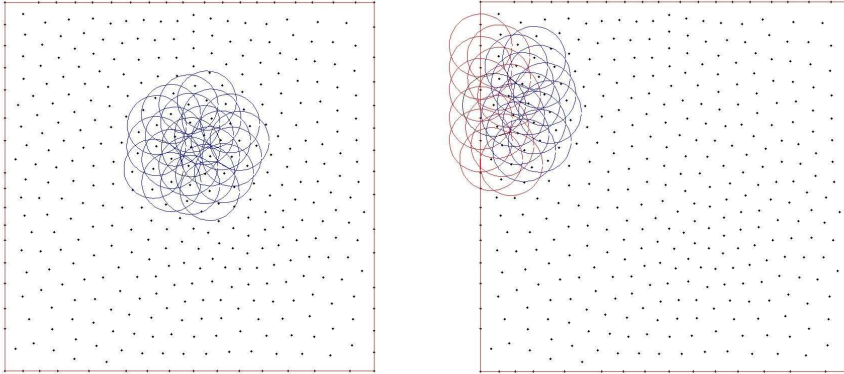

Figure 1: A point set $\{\mathbf{z}_i\}$ and an illustration of support overlaps given a cover of the domain with $r_i = 1.7/\sqrt{N}$. All patches Ω_{i_k} that intersect the two selected Ω_i are pictured. Patches that happen to overlap the boundary appear in red .

Following [6], on each patch we use a quartic spline window function

$$\omega(s) = \begin{cases} 1 - 6s^2 + 8s^3 - 3s^4 & \text{for} \quad 0 \le s \le 1, \\ 0 & \text{for} \quad s \ge 1, \end{cases}$$

and then define

$$\phi_i(\mathbf{z}) = \omega\left(\frac{|\mathbf{z} - \mathbf{z}_i|}{r_i}\right)$$

as building blocks for a Shepard partition of unity. That is, taken together, the functions

$$\psi_i(\mathbf{z}) = \frac{\phi_i(\mathbf{z})}{\sum_{j=1}^{N} \phi_j(\mathbf{z})}$$

yield a partition of unity of Ω, subordinate to $\mathscr{C}$. Note that the summation appearing in the denominator need only be conducted over indices j such that $\Omega_i \cap \Omega_j \ne \emptyset$; i.e., as depicted in Fig. 1. In the context of scalar function approximation, this immediately defines a global PU approximation space $\mathscr{V}^{h,0} := span\{\psi_i(\mathbf{z})\}$. The smoothness of the quartic spline window function yields the conformity of this space.

As detailed in the proof of convergence, partitioning unity provides the ability to transfer local approximation properties to the entire domain. For example, in analogy to p-refinement, global approximation can be enhanced by considering local spaces

$$\begin{aligned} \mathscr{V}_i^{h,q} := span\{\psi_i, (x - x_i)\psi_i, (y - y_i)\psi_i, \dots (x - x_i)^q\psi_i, \\ (x - x_i)^{q-1}(y - y_i)\psi_i, \dots, (y - y_i)^q\psi_i\} \, . \end{aligned} \tag{2.11}$$

Through direct summation, these give rise to the global PU approximation space

$$\mathscr{V}^{h,q} := \mathscr{V}_1^{h,q} \oplus \mathscr{V}_2^{h,q} \oplus \cdots \oplus \mathscr{V}_N^{h,q} \, . \tag{2.12}$$

Note that H^1 approximation requires $q \ge 1$.

Generalization to a vector setting follows immediately from introducing PU basis functions

$$\boldsymbol{\psi}_i^{(1)}(\mathbf{z}) = \begin{pmatrix} \psi_i(\mathbf{z}) \\ 0 \end{pmatrix} \quad \text{and} \quad \boldsymbol{\psi}_i^{(2)}(\mathbf{z}) = \begin{pmatrix} 0 \\ \psi_i(\mathbf{z}) \end{pmatrix} .$$

It is convenient, notationally, to suppress arguments and define 2×2 matrices

$$\Psi_i = \begin{pmatrix} \boldsymbol{\psi}_i^{(1)} & \boldsymbol{\psi}_i^{(2)} \end{pmatrix}$$

so that, using a constant coefficient vector $\boldsymbol{\alpha}_i = \begin{pmatrix} \alpha_i^{(1)} & \alpha_i^{(2)} \end{pmatrix}^t$,

$$\mathbf{u}^h = \sum_{i=1}^{N} \Psi_{r_i} \boldsymbol{\alpha}_i \quad \text{for any} \quad \mathbf{u}^h \in (\mathscr{V}^{h,0})^2 \, . \tag{2.13}$$

Clearly, we have a vector partition of unity in the sense that

$$I = \sum_{i=1}^{N} \Psi_{r_i} .$$

Consequently, for any $\mathbf{v} \in \left(H^k(\Omega)\right)^2$, note that

$$\mathbf{v} = \left(\sum_{i=1}^{N} \Psi_i\right) \mathbf{v} = \sum_{i=1}^{N} \Psi_i \mathbf{v} . \tag{2.14}$$

As done in the scalar case and in analogy to p-refinement, approximation on each Ω_i can be enhanced. For example, letting

$$\mathcal{Q}_i = span\left\{1, \frac{(x - x_i)}{r_i}, \frac{(y - y_i)}{r_i}\right\}$$

and taking the tensor product $\mathcal{Q}_i \otimes \mathcal{Q}_i$ leads to local approximation spaces

$$(\mathcal{V}_i^{h,1})^2 := span\left\{\boldsymbol{\psi}_i^{(1)}, \boldsymbol{\psi}_i^{(2)}, \frac{(x - x_i)}{r_i}\boldsymbol{\psi}_i^{(1)}, \frac{(y - y_i)}{r_i}\boldsymbol{\psi}_i^{(1)}, \frac{(x - x_i)}{r_i}\boldsymbol{\psi}_i^{(2)}, \frac{(y - y_i)}{r_i}\boldsymbol{\psi}_i^{(2)}\right\} . \tag{2.15}$$

Again, direct summation yields a global PU approximation space

$$(\mathcal{V}^{h,1})^2 := (\mathcal{V}_1^{h,1})^2 \oplus \cdots \oplus (\mathcal{V}_N^{h,1})^2 \tag{2.16}$$

subordinate to $\mathcal{C}$. Employing additional coefficient vectors, $\boldsymbol{\beta}_i$ and $\boldsymbol{\gamma}_i$, and folding these into a coefficient vector function, $\mathbf{U}_i \in \mathcal{Q}_i \otimes \mathcal{Q}_i$, allows us to write

$$\mathbf{u}^h = \sum_{i=1}^{N} \Psi_i \left[\boldsymbol{\alpha}_i + \frac{(x - x_i)}{r_i}\boldsymbol{\beta}_i + \frac{(y - y_i)}{r_i}\boldsymbol{\gamma}_i\right] = \sum_{i=1}^{N} \Psi_i \mathbf{U}_i \tag{2.17}$$

for any $\mathbf{u}^h \in (\mathcal{V}^{h,1})^2$. Hence, for example in the case that $\Omega \subset \mathbb{R}^2$, six unknowns are associated with each Ω_i. This space represents the simplest extension of the PUFEM for which convergence of the FOSLS formulation can be proven in the manner presented below. In general, the supplemental space $\mathcal{Q}$ can be built to suit, yielding global approximation spaces referred to below as $(\mathcal{V}^{h,q})^2$.

2.3. Convergence

To establish global convergence of a FOSLSPU formulation, certain local approximation is required [7]. We thus introduce the notion of a uniform Helmholtz partition of unity.

Definition 2.1. *A vector partition of unity, $(\mathcal{V}^{h,q})^2$, is uniform Helmholtz if, for any $\mathbf{u} \in (H^2(\Omega))^2$, there exist constants C_1, C_2, and C_3 independent of r_i such that there exist $\mathbf{W}_i \in \mathcal{Q}_i \otimes \mathcal{Q}_i$ satisfying*

(i) $\|\nabla \cdot (\mathbf{u} - \mathbf{W}_i)\|_{0,\,\Omega \cap \Omega_i} \leq 2C_1 r_i \|\mathbf{u}\|_{2,\,\Omega \cap \Omega_i}$;

(ii) $\|\nabla^\perp \cdot (\mathbf{u} - \mathbf{W}_i)\|_{0,\,\Omega \cap \Omega_i} \leq 2C_2 r_i \|\mathbf{u}\|_{2,\,\Omega \cap \Omega_i}$;

(iii) $\|\mathbf{u} - \mathbf{W}_i\|_{0,\,\Omega \cap \Omega_i} \leq 4C_3 r_i^2 \|\mathbf{u}\|_{2,\,\Omega \cap \Omega_i}$.

This definition suggests how convergence can be established, but first we generalize to the vector setting a lemma that appears in [7].

Lemma 2.1. *Define a maximum degree of covering overlap, M, such that $\forall\ \mathbf{z} \in \Omega$, $card\{i \mid \mathbf{z} \in \Omega_i\} \leq M$. Then, for any $f \in \left(\mathrm{H}^k(\Omega)\right)^2$ and any collection of $f_i \in \left(\mathrm{H}_0^k(\Omega \cap \Omega_i)\right)^2$, we have*

$$\sum_{i=1}^N \|f\|_{k,\,\Omega \cap \Omega_i}^2 \quad \leq \quad M \|f\|_{k,\,\Omega}^2 \tag{2.18}$$

and

$$\|\sum_{i=1}^N f_i\|_{k,\,\Omega}^2 \quad \leq \quad M \sum_{i=1}^N \|f_i\|_{k,\,\Omega \cap \Omega_i}^2 . \tag{2.19}$$

The proof using scalar norms that appears in [7] generalizes, componentwise, to vector norms without complication. We only remark that the second estimate neglects any specific treatment of each lenticular overlap $\Omega_i \cap \Omega_j$. Instead, the result follows from bounding each inner-product over such regions by an inner-product over all of Ω_i. This leads to the factor of M, suggesting some potential for refinement of this estimate given more careful analysis of a class of coverings. Of course, the maximum degree, M, is linked to the minimum degree of overlap; i.e., the minimum number of supports covering any given point in the domain. The latter characteristic of a covering impacts the smoothness of the functions $\{\psi_i(\mathbf{z})\}$, and thus also the accuracy of their integration.

We can now state and prove the following convergence result.

Theorem 2.1. *Let $(\mathcal{V}^{h,q})^2$ be a uniform Helmholtz partition of unity, with overlap degree M, constructed from a scalar partition of unity, $\{\psi_i\}$, that satisfies*

$$\|\psi_i\|_{0,\,\Omega \cap \Omega_i} = C_\infty , \tag{2.20}$$

$$\|\nabla \psi_i\|_{0,\,\Omega \cap \Omega_i} = \frac{C_g}{2r_i} , \tag{2.21}$$

for some constants C_∞ and C_g. Also, let

$$\mathbf{u}^h := \arg \min_{\mathbf{v}^h \in (\mathcal{V}^{h,q})^2} \mathcal{J}(\mathbf{v}^h; f) . \tag{2.22}$$

Then, there exists a constant C, depending only on C_1, C_2, C_3, C_∞, and C_g, such that

$$\mathcal{J}(\mathbf{u} - \mathbf{u}^h; 0) \leq 2CM r_{max} \|\mathbf{u}\|_{2,\,\Omega} , \tag{2.23}$$

where $r_{max} = \max_i\{r_i\}$.

Proof. First, via triangle inequality,

$$\mathscr{J}(\mathbf{u} - \mathbf{u}^h; 0) \le \mathscr{J}(\mathbf{u} - \mathbf{w}^h; 0) + \mathscr{J}(\mathbf{w}^h - \mathbf{u}^h; 0) \tag{2.24}$$

for any $\mathbf{w}^h \in (\mathscr{V}^{h,q})^2$. In particular, set $\mathbf{w}^h = \sum_{i=1}^N \Psi_i \mathbf{W}_i$, where $\mathbf{W}_i$ is that which is guaranteed by the uniform Helmholtz property. Then,

$$\begin{aligned}
\left(\mathscr{J}(\mathbf{w}^h - \mathbf{u}^h; 0)\right)^2 &= \mathscr{F}(\mathbf{w}^h - \mathbf{u}^h, \mathbf{w}^h - \mathbf{u}^h) \\
&= \mathscr{F}(\mathbf{w}^h - \mathbf{u} + \mathbf{u} - \mathbf{u}^h, \mathbf{w}^h - \mathbf{u}^h) \\
&= \mathscr{F}(\mathbf{w}^h - \mathbf{u}, \mathbf{w}^h - \mathbf{u}^h) \\
&\le \mathscr{J}(\mathbf{w}^h - \mathbf{u}^h; 0)\mathscr{J}(\mathbf{u} - \mathbf{w}^h; 0) \tag{2.25}
\end{aligned}$$

by virtue of the orthogonality condition on $\mathbf{u} - \mathbf{u}^h$ that follows from (2.22). Thus, since

$$\mathscr{J}(\mathbf{u} - \mathbf{u}^h; 0) \le 2\mathscr{J}(\mathbf{u} - \mathbf{w}^h; 0), \tag{2.26}$$

it suffices to bound the quantity $\mathscr{J}(\mathbf{u} - \mathbf{w}^h; 0)$ in terms of the radii of supports Ω_i. The above lemma, combined with the uniform Helmholtz property, provide the bound as follows. First, property (2.14) yields

$$\begin{aligned}
\left(\mathscr{J}(\mathbf{u} - \mathbf{w}^h; 0)\right)^2 &= \mathscr{F}(\mathbf{u} - \mathbf{w}^h, \mathbf{u} - \mathbf{w}^h) \\
&= \|\nabla \cdot (\mathbf{u} - \mathbf{w}^h)\|_{0,\Omega}^2 + \|\nabla^\perp \cdot (\mathbf{u} - \mathbf{w}^h)\|_{0,\Omega}^2 \\
&= \|\nabla \cdot \sum_{i=1}^N \Psi_i(\mathbf{u} - \mathbf{W}_i)\|_{0,\Omega}^2 + \|\nabla^\perp \cdot \sum_{i=1}^N \Psi_i(\mathbf{u} - \mathbf{W}_i)\|_{0,\Omega}^2. \tag{2.27}
\end{aligned}$$

Then, separately appealing to the second estimate in Lemma 2.1 leads to

$$\begin{aligned}
&\|\nabla \cdot \sum_{i=1}^N \Psi_i(\mathbf{u} - \mathbf{W}_i)\|_{0,\Omega} \\
&\le \|\sum_{i=1}^N \psi_i \nabla \cdot (\mathbf{u} - \mathbf{W}_i)\|_{0,\Omega} + \|\sum_{i=1}^N \nabla\psi_i \cdot (\mathbf{u} - \mathbf{W}_i)\|_{0,\Omega} \\
&\le \left(M \sum_{i=1}^N \|\psi_i \nabla \cdot (\mathbf{u} - \mathbf{W}_i)\|_{0,\Omega\cap\Omega_i}^2 \right)^{1/2} + \left(M \sum_{i=1}^N \|\nabla\psi_i \cdot (\mathbf{u} - \mathbf{W}_i)\|_{0,\Omega\cap\Omega_i}^2 \right)^{1/2} \tag{2.28}
\end{aligned}$$

and

$$\begin{aligned}
&\|\nabla^\perp \cdot \sum_{i=1}^N \Psi_i(\mathbf{u} - \mathbf{W}_i)\|_{0,\Omega} \\
&\le \|\sum_{i=1}^N \psi_i \nabla^\perp \cdot (\mathbf{u} - \mathbf{W}_i)\|_{0,\Omega} + \|\sum_{i=1}^N \nabla^\perp\psi_i \cdot (\mathbf{u} - \mathbf{W}_i)\|_{0,\Omega} \\
&\le \left(M \sum_{i=1}^N \|\psi_i \nabla^\perp \cdot (\mathbf{u} - \mathbf{W}_i)\|_{0,\Omega\cap\Omega_i}^2 \right)^{1/2} + \left(M \sum_{i=1}^N \|\nabla^\perp\psi_i \cdot (\mathbf{u} - \mathbf{W}_i)\|_{0,\Omega\cap\Omega_i}^2 \right)^{1/2}. \tag{2.29}
\end{aligned}$$

Then, bounds (2.20-2.21) and the uniform Helmholtz property provide that

$$\|\nabla \cdot \sum_{i=1}^{N} \Psi_i(\mathbf{u} - \mathbf{W}_i)\|_{0,\Omega}$$

$$\leq \left(MC_\infty^2 \sum_{i=1}^{N} \|\nabla \cdot (\mathbf{u} - \mathbf{W}_i)\|_{0,\Omega \cap \Omega_i}^2 \right)^{1/2} + \left(MC_g^2 \sum_{i=1}^{N} \frac{1}{4r_i^2} \|(\mathbf{u} - \mathbf{W}_i)\|_{0,\Omega \cap \Omega_i}^2 \right)^{1/2}$$

$$\leq \left(4MC_\infty^2 C_1^2 r_{max}^2 \sum_{i=1}^{N} \|\mathbf{u}\|_{2,\Omega \cap \Omega_i}^2 \right)^{1/2} + \left(4MC_g^2 C_3^2 r_{max}^2 \sum_{i=1}^{N} \|\mathbf{u}\|_{2,\Omega \cap \Omega_i}^2 \right)^{1/2} \tag{2.30}$$

and

$$\|\nabla^\perp \cdot \sum_{i=1}^{N} \Psi_i(\mathbf{u} - \mathbf{W}_i)\|_{0,\Omega}$$

$$\leq \left(MC_\infty^2 \sum_{i=1}^{N} \|\nabla^\perp \cdot (\mathbf{u} - \mathbf{W}_i)\|_{0,\Omega \cap \Omega_i}^2 \right)^{1/2} + \left(MC_g^2 \sum_{i=1}^{N} \frac{1}{4r_i^2} \|(\mathbf{u} - \mathbf{W}_i)\|_{0,\Omega \cap \Omega_i}^2 \right)^{1/2}$$

$$\leq \left(4MC_\infty^2 C_2^2 r_{max}^2 \sum_{i=1}^{N} \|\mathbf{u}\|_{2,\Omega \cap \Omega_i}^2 \right)^{1/2} + \left(4MC_g^2 C_3^2 r_{max}^2 \sum_{i=1}^{N} \|\mathbf{u}\|_{2,\Omega \cap \Omega_i}^2 \right)^{1/2}. \tag{2.31}$$

Finally, employing the first estimate of Lemma 2.1 and combining each of the above according to (2.27) implies that

$$\mathscr{I}(\mathbf{u} - \mathbf{w}^h; 0) \leq \left([C_\infty C_1 + C_g C_3]^2 + [C_\infty C_2 + C_g C_3]^2 \right)^{1/2} 2Mr_{max} \|\mathbf{u}\|_{2,\Omega}, \tag{2.32}$$

so that setting $C = \left([C_\infty C_1 + C_g C_3]^2 + [C_\infty C_2 + C_g C_3]^2 \right)^{1/2}$ completes the proof. □

Accounting for inexact integration entails defining a projection of f,

$$f^h := \arg \min_{w^h \in \mathscr{V}^h} \|f - w^h\|_{L^2(\Omega)}, \tag{2.33}$$

that satisfies

$$\left\langle f - f^h, \psi_{r_i} \right\rangle_{0,\Omega} = 0, \forall i. \tag{2.34}$$

Then, as approximate solution to (2.1-2.4), we seek

$$\mathbf{u}^h := \arg \min_{\mathbf{w}^h \in (\mathscr{V}^{h,1})^2} \mathscr{I}(\mathbf{w}^h; f^h). \tag{2.35}$$

Well-posedness of (2.35) follows from extending (2.24) to include an additional error term $\|f - f^h\|$, and subsequently employing the same line of proof.

3. Numerical demonstration

3.1. Boundary functionals

To demonstrate the above, consider the Neumann problem

$$-\nabla \cdot \mathbf{u} = f \qquad \text{in } \Omega, \tag{3.1}$$

$$\nabla \times \mathbf{u} = \mathbf{0} \qquad \text{in } \Omega, \tag{3.2}$$

$$\mathbf{n} \cdot \mathbf{u} = g \qquad \text{on } \Gamma, \tag{3.3}$$

and the more general FOSLS functional with boundary terms

$$\mathscr{I}_{bdy'}(\mathbf{u}; f) := \left(\|\nabla \cdot \mathbf{u} + f\|_{0,\Omega}^2 + \|\nabla \times \mathbf{u}\|_{0,\Omega}^2 + \|\mathbf{n} \cdot \mathbf{u} - g\|_{-1/2,\Gamma}^2 \right)^{1/2}. \tag{3.4}$$

Practically, in lieu of the Sobolev boundary norm, we use an appropriately weighted L^2-norm on the boundary and define

$$\mathscr{I}_{bdy}(\mathbf{u}; f, g) := \left(\|\nabla \cdot \mathbf{u} + f\|_{0,\Omega}^2 + \|\nabla \times \mathbf{u}\|_{0,\Omega}^2 + \frac{1}{r}\|\mathbf{n} \cdot \mathbf{u} - g\|_{0,\Gamma}^2 \right)^{1/2}. \tag{3.5}$$

Hence, we seek

$$\mathbf{u}^h := \arg \min_{\mathbf{w}^h \in (\mathscr{V}^{h,1})^2} \mathscr{I}_{bdy}(\mathbf{w}^h; f^h, g^h). \tag{3.6}$$

In the event that a chosen cover consists of patches with non-uniform radii, this weighting should be enacted during assembly in a consistent fashion. Also, note that unlike standard finite elements, interior nodes contribute to the solution at the boundary. That is, PU basis elements do not have the kronecker delta property and the unknown associated with a node on the boundary is not the function value at that node.

As discussed in the introduction, assembly of the discrete problem (3.6) is performed by quadrature on a disc [8], translated and dilated to each Ω_i. The symmetric part of the resulting matrix is then taken. Integration remains a significant challenge to the efficacy of meshfree methods. We have resorted to a 64pt scheme on each patch to achieve the accuracy apparent in the below selected examples. Use of a 16pt alters diagonal entries of the stiffness matrix significantly (by 10-50 %), depending on the extent of overlap in the cover $\mathscr{C}$ and its impact on the regularity of the basis elements ψ_i.

3.2. Selected examples

The three examples presented correspond, respectively, with the following exact solutions

$$\mathbf{u} = \begin{pmatrix} x(1-x) \\ y(1-y) \end{pmatrix}, \tag{3.7}$$

$$\mathbf{u} = \begin{pmatrix} x \\ y \end{pmatrix}, \tag{3.8}$$

and

$$\mathbf{u} = \begin{pmatrix} k\pi \cos(k\pi x)\sin(l\pi y) \\ l\pi \sin(k\pi x)\cos(l\pi y) \end{pmatrix} \text{ with } k = 1.2 \text{ and } l = 2.3 \,. \tag{3.9}$$

In each case, f and g are set accordingly. Fig. 2 depicts solutions using only a vector PU while Fig. 3 shows results using a Helmholtz PU.

Clearly, in light of Table 1, these elementary examples present significant practical computational challenges. The theoretical advantage to constructing Helmholtz partition of unity is off-set by severe conditioning of the resulting linear systems. Helmholtz PU yield stiffness matrices with condition numbers $10^6 - 10^7$, compared to $10^2 - 10^3$ for the simple vector PU in the case $N = 400$; note that these discretizations involve 2400 and 800 unknowns, respectively. A supplemental least-squares PU approach to mesh refinement may, in practice, present similar drawbacks that derive from the prohibitive need for precise integration over lenticular regions.

Table 1: Example 1: Convergence employing $(\mathcal{V}^{h,0})^2$ and $(\mathcal{V}^{h,1})^2$ for two different radii, set as indicated to define the covering.

Discretization	N	$r_i = 1.7/\sqrt{N}$	$L^2(\Omega)$	$\mathcal{J}_n(\mathbf{u}^h; f^h, g^h)$
$(\mathcal{V}^{h,0})^2$	64	.2125	1.604e-03	1.419e-01
	256	.1062	1.071e-03	4.013e-02
	400	.0854	9.198e-04	2.094e-02
$(\mathcal{V}^{h,1})^2$	64	.2125	3.969e-02	3.893e-01
	256	.1062	3.359e-02	3.387e-01
	400	.0854	4.186e-02	4.059e-01
		$r_i = 2.3/\sqrt{N}$		
$(\mathcal{V}^{h,0})^2$	64	.2875	1.435e-03	1.170e-01
	256	.1437	7.597e-04	1.678e-01
	400	.1150	6.441e-04	1.736e-01
$(\mathcal{V}^{h,1})^2$	64	.2125	2.881e-02	2.384e-01
	256	.1062	2.668e-02	3.037e-01
	400	.0854	2.688e-02	3.209e-01

3.3. Adaptive enrichment algorithm

Given an approximate solution $\mathbf{u}^h$, local FOSLS functional values

$$\mathcal{J}_i(\mathbf{u}^h; f^h) := \left(\|\nabla \cdot \mathbf{u}^h + f^h\|_{0,\Omega_i}^2 + \|\nabla^\perp \cdot \mathbf{u}^h\|_{0,\Omega_i}^2 \right)^{1/2} \,. \tag{3.10}$$

may be computed through submatrix-subvector multiplications. This suggests some utility in determining an approximately minimal subcover $\mathcal{C}_0 \subset \mathcal{C}$ when defining $\mathcal{C}$ initially. Then, to quantify further enrichment of the point set using local FOSLS estimates, a simple way to define a density function is to impose

$$\rho_{\mathbf{u}^h}(x_i, y_i) = \mathcal{J}_i(\mathbf{u}^h; f^h, g^h) \quad \forall i \text{ such that } \Omega_i \in \mathcal{C}_0. \tag{3.11}$$

(a)   (b)

(c)   (d)

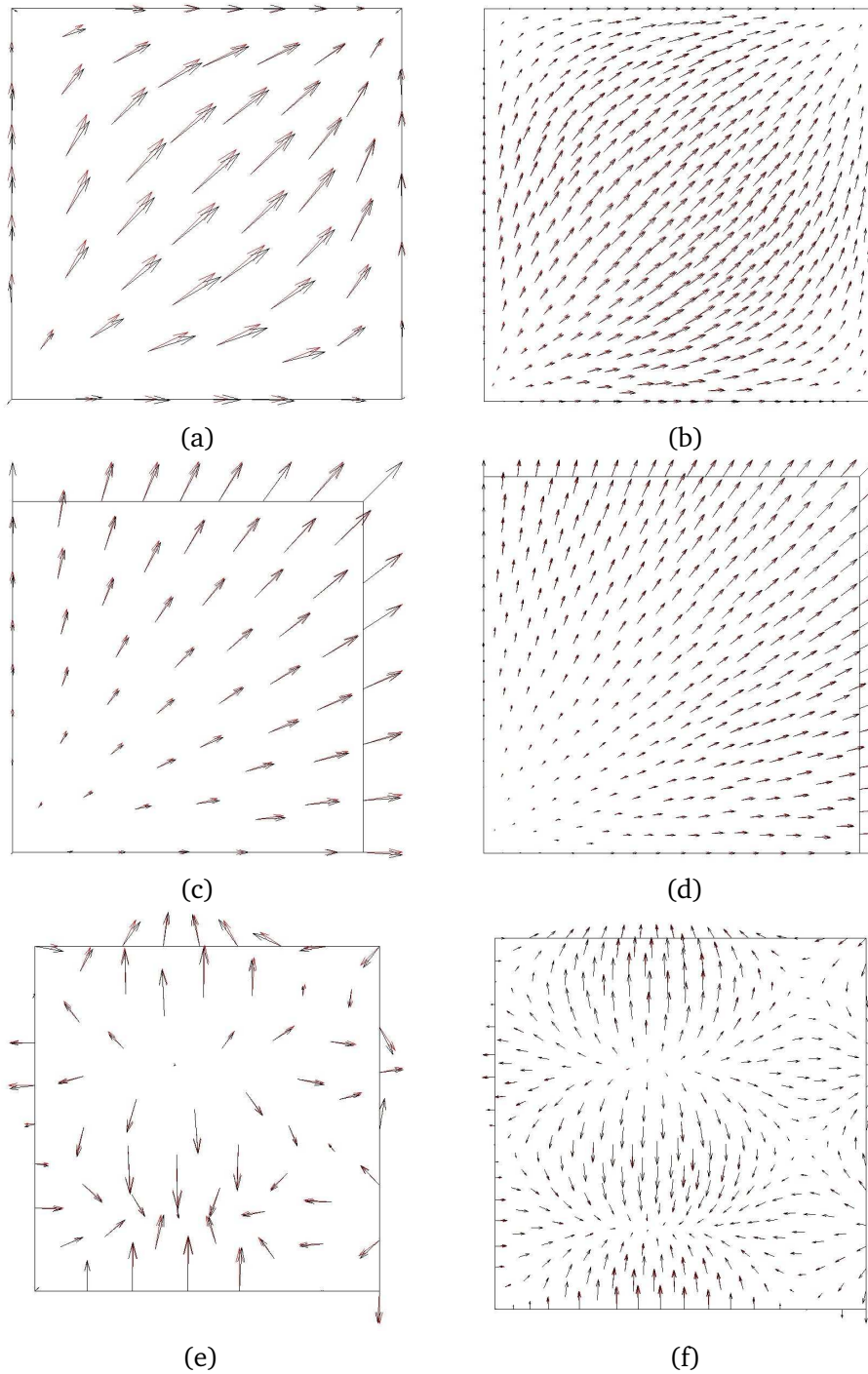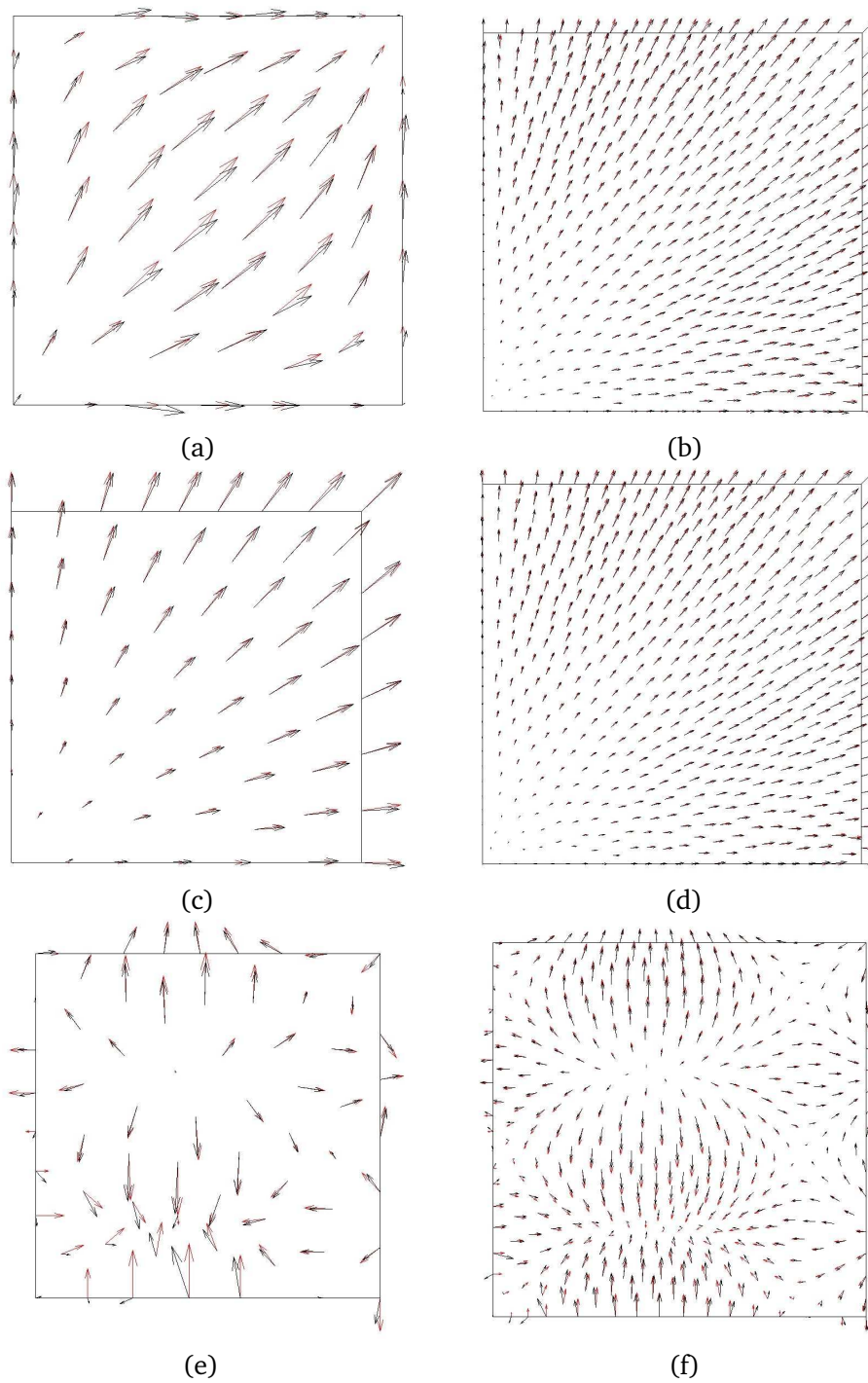(e)   (f)

Figure 2: For (a)-(b) Example 1, (c)-(d) Example 2, and (e)-(f) Example 3, the exact solution is shown in red and the computed solution is shown in black. The cases $N = 64$ and $N = 400$ using $(\mathscr{V}^{h,0})^2$ are depicted.

Figure 3: For (a)-(b) Example 1, (c)-(d) Example 2, and (e)-(f) Example 3, the exact solution is shown in red and the computed solution is shown in black. The cases $N = 64$ and $N = 400$ using $(\mathscr{V}^{h,1})^2$ are depicted.
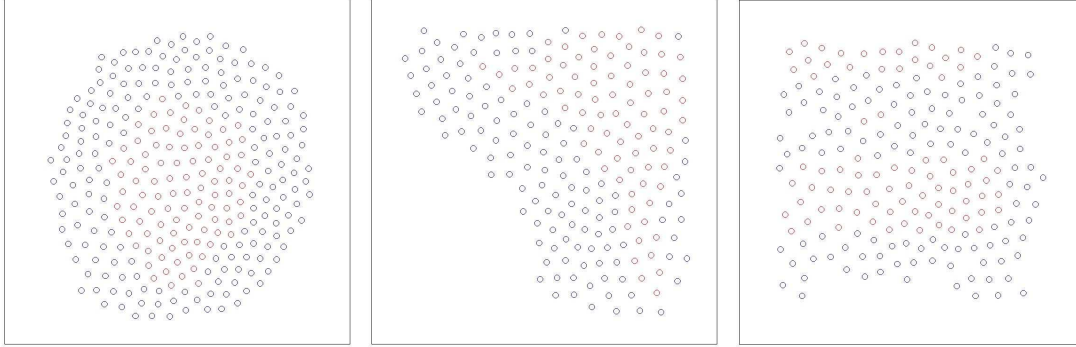
Figure 4: Among the interior local FOSLS functional values, the largest quintile are depicted in red for each of the three examples. The remainder, in blue, are above the average local FOSLS functional value.

 Provided convergence can be improved in practice, this suggests the following simplistic algorithm for meshfree enrichment:

---

1. Select an initially-coarse point set and covering to construct a Helmholtz partition of unity $\mathscr{V}^{h,q}$.

2. Compute $\mathbf{u}^h$ by solving (3.6).

3. Evaluate local estimates (3.10) $\forall\, i \in \mathscr{C}_0$, as visualized in Fig. 4.

4. Define a density function $\rho_{\mathbf{u}^h}(x, y)$ satisfying (3.11) and assess equi-distribution of error.

5. If needed, supplement the initial point set in targeted patches subject to $\rho_{\mathbf{u}^h}(x, y)$ and repeat.

---

4. Concluding remarks

Given the compromises in efficiency that accompany a truly meshfree approach, its primary appeal may be as a conformal supplement to more-standard discretizations. In principle, this could be done precisely within a least-squares setting, whether the mesh-free flexibility is utilized to resolve multiscale phenomena or to optimize least-squares approaches to local mesh adaptation [9]. Integration, however, and its impact on conditioning, remains a concern.

Beyond mechanics and classical PDE systems, application of PU methods to dynamic cell-centered biological simulations may hold special promise [10, 11]. This is due to natural interest in either moving (cell migration), eliminating (cell death), or adding (cell division) subsets of points used to build multilevel — with respect to biological organization — descriptions of various molecular factors and their impact on cell proliferation, cell differentiation, and cell death in tissue.

References

[1] S. Li and W. K. Liu, *Meshfree and particle methods and their applications*, Appl. Mech. Rev., 55 (2002), pp. 1–34.

[2] T.-P. Fries and H. G. Matthies, *Classification and Overview of Meshfree Methods*, Technical Report, Institure of Scientific Computing, Technical University Braunschweig, 2003.

[3] Q. Du, M. Gunzburger, and L. Ju, *Meshfree, probabilistic determination of point sets and support regions for meshless computing*, Comput. Meth. Appl. Mech. Eng., 191 (2002), pp. 1349–1366.

[4] M. Berndt, T. A. Manteuffel, and S. F. McCormick, *Analysis of first-order system least squares (FOSLS) for elliptic problems with discontinuous coefficients: Part I*, SIAM J. Numer. Anal., 43 (2006), pp. 386–408.

[5] X. K. Zhang, K.-C. Kwon, and S.-K. Youn, *The least-squares meshfree method for the steady incompressible viscous flow*, J. Comput. Phys., 206 (2005), pp. 182–207.

[6] C. A. Duarte and J. T. Oden, *H-p Clouds – an h-p meshless method*, Numer. Meth. PDEs, 12 (1996), pp. 673–705.

[7] I. Babuska and J. M. Melenk, *The partition of unity method*, Comput. Meth. Appl. Mech. Eng., 40 (1997), pp. 727–758.

[8] A. Stroud and D. Secrest, *Gaussian Quadrature Formulas*, Prentice Hall, 1966.

[9] P. Bochev, G. Liao, and G. Pena, *Analysis and computation of adaptive moving grids by deformation*, Numer. Meth. PDEs, 12 (1996), pp. 489–506.

[10] B. P. Ayati, G. F. Webb, and A. R. A. Anderson, *Computational methods and results for structured multiscale models of tumor invasion*, SIAM Multiscale Model. Simul., 5 (2006), pp. 1–20.

[11] H. R. MacMillan, *On the potential for explanatory modeling of cellular decisions during neurogenesis*, Bull. Math. Bio., to appear.